

On-line Inertia Estimation of Virtual Power Plants

Weilin Zhong¹, Georgios Tzounas¹, Muyang Liu², and Federico Milano¹

¹School of Electrical & Electronic Engineering, University College Dublin, Ireland

²School of Electrical Engineering, Xinjiang University, China

weilin.zhong@ucdconnect.ie, georgios.tzounas@ucd.ie, muyang.liu@xju.edu.cn, federico.milano@ucd.ie

Abstract—This paper presents an on-line estimation method to track the equivalent, time-varying inertia provided by Virtual Power Plants (VPPs). The proposed method relies on the estimation of the rate of change of the active and reactive power at the point of connection of the VPP with the rest of the grid and provides, as a byproduct, an estimation of the VPP's internal equivalent reactance. The accuracy of the proposed method is first validated by estimating the rotational inertia of Synchronous Machines (SMs), and then tested for a VPP, based on a comprehensive case study carried out based on the WSCC 9-bus test system.

Index Terms—Inertia estimation, power system dynamics, Virtual Power Plant (VPP), virtual inertia, equivalent reactance.

I. INTRODUCTION

A. Motivation

The VPP concept refers to the aggregation of several devices, including Distributed Energy Resources (DERs), Energy Storage Systems (ESSs), and flexible loads, coordinated to operate as a single generating unit [1]. In most cases, VPPs consist of devices connected to the grid through power electronic converters. This kind of non-synchronous VPPs contributes to the reduction of the overall available rotational inertia in the system which, in turn, may lead to large frequency variations and threat the dynamic performance and stability of the grid [1], [2]. On the other hand, if properly controlled, VPPs can provide, as an ancillary service, an inertial response that is similar to that provided by conventional SMs [3]. The goal of this paper is to provide a novel method to estimate the equivalent inertia provided by VPPs, a tool that can help system operators to better plan, monitor, and control their network.

B. Literature Review

In a conventional power system, inertia is naturally provided by SMs, as a consequence of the kinetic energy stored in the masses of their rotors. The mechanical inertia of SMs, being the mechanism that counters frequency variations during the first instants after an active power imbalance in the network, has played a crucial role in maintaining the stability of

traditional power systems. The ongoing gradual substitution of SMs by non-synchronous devices reduces significantly the amount of mechanical inertia in the system, thus leading in larger frequency and Rate of Change of Frequency (RoCoF) variations after a disturbance and increasing the risk of a system collapse. Hence, there has been intense research in the last decade on the role of inertia, as well as on techniques to monitor and estimate the inertia of the system. With this regard, measurement-based methods have been proposed in the literature for both off-line [4], [5] and on-line [6]–[8] estimation of the available mechanical inertia at a given time.

Non-synchronous devices do not provide mechanical inertia to the system but the controls of their power converters can be designed so that they emulate the inertial response of SMs, leading to the concept of *equivalent* or *virtual* inertia. It is relevant to note that, in contrast to the inertia constant of a SM, the virtual inertia provided by a non-synchronous device may be time-varying.

A number of recent studies have been conducted on the use of virtual inertia as an ancillary service to improve the stability of power systems, e.g. see [9], [10]. Other studies provide techniques for estimating and monitoring the equivalent inertia provided by non-synchronous devices, for example, see [8], [11], [12]. In particular, [11] presents an estimator to on-line track the physical and equivalent inertia of synchronous and non-synchronous devices, respectively. In [12], the authors improve the numerical stability of the estimator in [11] and extend it to also track the droop gain of fast frequency regulation.

This work is concerned with the estimation of the equivalent inertia provided by VPPs. A limitation of most currently existing techniques in the literature is that they work well only when applied to estimate the inertia of a single device. We thus take advantage of the concepts presented in [11]–[13] to provide a method to on-line track the equivalent inertia of a subnetwork comprising several devices, and apply this method to VPPs.

C. Contributions

The contributions of this paper are the following.

- A technique for the on-line estimation of the equivalent inertia provided by VPPs.
- As a byproduct of the technique above, a formula to estimate the equivalent reactance of any device/subnetwork connected to the power system, based on bus voltage and reactive power measurements.

This work was supported by Science Foundation Ireland, by funding W. Zhong and F. Milano under project ESIPP, grant no. SFI/15/SPP/E3125; and by the European Commission, by funding G. Tzounas and F. Milano under the project EdgeFLEX, grant agreement no. 883710.

The contributions of the paper are supported by a comprehensive study that evaluates the proposed inertia estimation method under different scenarios, based on simulations conducted on the WSCC 9-bus system.

D. Organization

The remainder of the paper is organized as follows. Section II outlines the on-line inertia estimation of synchronous and non-synchronous devices, based on results from the recent literature, particularly from [11] and [12]. The proposed method to estimate the equivalent inertia and the equivalent internal reactance of VPPs is described in Section III. The case study is discussed in Section IV based on the WSCC 9-bus system. Conclusions are drawn and future work is outlined in Section V.

II. BACKGROUND

The inertia constant affects the dynamics of SMs through the swing equation, as follows [14]:

$$M_G \dot{\omega}_G = p_m - p_G - D_G(\omega_G - \omega_o), \quad (1)$$

where M_G is the machine's starting time, which is twice the inertia constant, i.e., $M_G = 2H_G$; ω_G is the machine's rotor speed and $\dot{\omega}_G$ denotes its time derivative; p_m is the mechanical power; p_G is the electrical power that the machine injects to the grid; D_G is the damping coefficient; and ω_o is the machine's rated rotor speed.

For the sake of derivation, it is convenient to split the mechanical power into the following components:

$$p_m = p_{\text{PFC}} + p_{\text{SFC}} + p_{\text{UC}}, \quad (2)$$

where p_{PFC} is the active power regulated by the Primary Frequency Control (PFC), typically achieved through the Turbine Governor (TG); p_{SFC} is the active power regulated by the Secondary Frequency Control (SFC), typically achieved through an Automatic Generation Control (AGC) scheme; and p_{UC} is the power set point as defined by the solution of the unit commitment problem.

Putting together (1) and (2) and differentiating with respect to time, one has:

$$M_G \ddot{\omega}_G = \dot{p}_{\text{PFC}} + \dot{p}_{\text{SFC}} + \dot{p}_{\text{UC}} - \dot{p}_G - D_G \dot{\omega}_G. \quad (3)$$

In the time scale of the inertial response of the SM, we can assume that $\dot{p}_{\text{UC}} \approx 0$, $\dot{p}_{\text{SFC}} \approx 0$, as well as that $|\dot{p}_{\text{PFC}}| \ll |\dot{p}_G|$. Assuming, in addition, that $D_G \approx 0$, one gets that:

$$M_G \approx -\frac{\dot{p}_G}{\ddot{\omega}_G}. \quad (4)$$

Equation (4) can be extended to also take into account non-synchronous devices, under the assumption that their power converters are controlled to provide a dynamic response that is in the same time scale with the inertial response of SMs. Then, one can write [12]:

$$M_{D,h} \approx -\frac{\dot{p}'_h}{\ddot{\omega}_{D,h}}, \quad (5)$$

where $M_{D,h}$ is the *equivalent* inertia that a device connected to bus h provides following a contingency and $\omega_{D,h}$ is its internal frequency; \dot{p}'_h can be estimated based on Phasor Measurement Unit (PMU) measurements; and [11]:

$$\omega_{D,h} = \Delta\omega_h - x_{D,h} \dot{p}'_h, \quad (6)$$

where $x_{D,h}$ is the equivalent reactance of the device; \dot{p}'_h is the derivative of the quota of the active power that can be used to regulate the frequency at bus h [11]; and $\Delta\omega_h$ is the frequency deviation at the bus to which the device is connected.

Equation (5) shows numerical issues, e.g. if the denominator $\ddot{\omega}_{D,h}$ changes sign and hence cross zero during the first seconds following the disturbance, thus leading to a singularity. Then, $\ddot{\omega}_G = 0$ in steady state. To avoid this singularity, the third and fourth authors of this paper presented the following differential equation to determine $M_{D,h}$ [12]:

$$T_M \dot{M}_{D,h} = \gamma(\ddot{\omega}_{D,h}) (M_{D,h} \ddot{\omega}_{D,h} + \dot{p}'_h), \quad (7)$$

where the time constant T_M opposes the change of $M_{D,h}$; the function $\gamma(y)$ is defined as follows [12]:

$$\gamma(y) = \begin{cases} -1, & y \geq \epsilon_y, \\ 0, & -\epsilon_y < y < \epsilon_y, \\ 1, & y \leq -\epsilon_y, \end{cases} \quad (8)$$

where ϵ_y is a positive and $(-\epsilon_y, \epsilon_y)$ is a small deadband to avoid chattering around the equilibrium. A proper choice of ϵ_y can both improve the accuracy of the function $\gamma(y)$ and reduce the impact of noise. A good selection of ϵ_y is $\epsilon_y \in [10^{-7}, 10^{-5}]$.

III. INERTIA ESTIMATION OF VPPS

The estimator (6)-(7) works well for a single device connected to a bus of a power network, and provided that the value of the reactance $x_{D,h}$ is known. A VPP aggregates several resources that may span multiple buses and/or areas of the grid and, thus, how to define $x_{D,h}$ to account for the total equivalent reactance of a VPP is a challenging task.

In this section, we first provide a technique to estimate $x_{D,h}$, based on measurements of the reactive power and using the concept of the *complex frequency* presented in [13]. Then, we provide a generalized formula that can estimate the equivalent inertia of any subnetwork that consists of many resources, and hence also the equivalent inertia of a VPP.

The starting point is the well-known power flow equations that describe the complex power injections at a network with n buses, say $\bar{s} \in \mathbb{C}^{n \times 1}$, as follows:

$$\begin{aligned} \bar{s}(t) &= \mathbf{p}(t) + j\mathbf{q}(t) \\ &= \bar{\mathbf{v}}(t) \circ \bar{\mathbf{i}}^*(t) \\ &= \bar{\mathbf{v}}(t) \circ (\bar{\mathbf{Y}} \bar{\mathbf{v}}(t))^*, \end{aligned} \quad (9)$$

where $\mathbf{p}, \mathbf{q} \in \mathbb{C}^{n \times 1}$ are the column vectors of the bus active and reactive power injections, respectively; $\bar{\mathbf{v}}, \bar{\mathbf{i}} \in \mathbb{C}^{n \times 1}$ are the vectors of bus voltages and current injections, respectively; $\bar{\mathbf{Y}} \in \mathbb{C}^{n \times n}$ is the network admittance matrix; \circ denotes the element-wise multiplication; and $*$ indicates the conjugate.

Rewriting (9) in an element-wise notation and omitting for simplicity the time dependency, the h -th elements of \mathbf{p} and \mathbf{q} can be written as:

$$\begin{aligned} p_h &= \sum_{k=1}^n p_{h,k} = \sum_{k=1}^n v_h v_k (G_{h,k} \cos \theta_{h,k} + B_{h,k} \sin \theta_{h,k}), \\ q_h &= \sum_{k=1}^n q_{h,k} = \sum_{k=1}^n v_h v_k (G_{h,k} \sin \theta_{h,k} - B_{h,k} \cos \theta_{h,k}), \end{aligned} \quad (10)$$

where $p_{h,k}$, $q_{h,k}$ are the active and reactive power flows, respectively, from bus h to bus k ; $G_{h,k}$ and $B_{h,k}$ are the real and imaginary parts of the (h, k) element of \mathbf{Y} , i.e. $\bar{Y}_{h,k} = G_{h,k} + jB_{h,k}$; v_k is the voltage magnitude at bus k ; and $\theta_{h,k} = \theta_h - \theta_k$, where θ_h and θ_k are the voltage phase angles at buses h and k , respectively.

Differentiation of (10) gives:

$$dp_h = \sum_{k=1}^n \frac{\partial p_h}{\partial \theta_{h,k}} d\theta_{h,k} + \sum_k^n \frac{\partial p_h}{\partial v_k} dv_k \equiv dp'_h + dp''_h, \quad (11)$$

$$dq_h = \sum_{k=1}^n \frac{\partial q_h}{\partial \theta_{h,k}} d\theta_{h,k} + \sum_{k=1}^n \frac{\partial q_h}{\partial v_k} dv_k \equiv dq'_h + dq''_h, \quad (12)$$

where dp'_h and dq'_h are the quotas of the active and reactive power that depend on bus voltage phase angle variations; dp''_h and dq''_h are the quotas of active and reactive power that depend on bus voltage magnitude variations. Considering differentiation with respect to time, (12) can be rewritten as:

$$\dot{q}_h = \dot{q}'_h + \dot{q}''_h. \quad (13)$$

Note that \dot{q}''_h is the component that varies the most when the reactive power at bus h is regulated, whereas the contribution of \dot{q}'_h to the reactive power regulation is negligible. Applying the complex frequency formula proposed in [13], \dot{q}''_h can be conveniently expressed using a matrix form, as follows:

$$\dot{\mathbf{q}}'' \approx \mathbf{B}'' \boldsymbol{\varrho}, \quad (14)$$

where \mathbf{B}'' is the imaginary part of the network admittance matrix and $\boldsymbol{\varrho}$ defines that the magnitude of the voltage is expressed as a function whose derivative is equal to the function itself. The h -th element of $\boldsymbol{\varrho}$ can be expressed as follows [13]:

$$\varrho_h \equiv \frac{\dot{v}_h}{v_h}. \quad (15)$$

Let us assume that a subnetwork comprising possibly several devices (e.g. a VPP) is connected to bus h of the network. An example is shown in Fig. 1, where a VPP is connected in antenna to the grid. Then, applying (14) to bus h and following from the above discussion, we can write:

$$\dot{q}_h \approx \dot{q}''_h \approx B''_{h,h} \varrho_h + \sum_{k=1}^n B''_{h,k} \varrho_k, \quad (16)$$

where $B''_{h,k}$ is the imaginary part of the (h, k) element of the network admittance matrix, and $B''_{D,h}$ is the equivalent internal reactance of the subnetwork. B''_h can be obtained from:

$$B''_h = B''_{D,h} + B''_{h,h} + \sum_{k=1}^n B''_{h,k}, \quad (17)$$

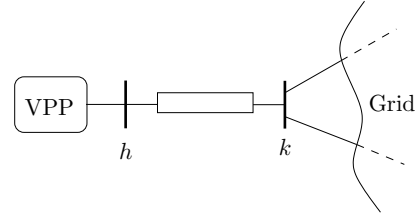


Fig. 1: VPP connected in antenna to the grid.

where $B''_{h,h}$ is the shunt susceptance at bus h . Merging (16) and (17) gives the following formula to estimate the equivalent susceptance of the subnetwork connected to bus h :

$$B''_{D,h} = \frac{\dot{q}''_h - \sum_{k=1}^n B''_{h,k} \varrho_k}{\varrho_h} - \sum_{k=1}^n B''_{h,k} - B''_{h,h}. \quad (18)$$

The equivalent reactance of the subnetwork $x_{D,h}$ can be obtained from the reciprocal of $B''_{D,h}$, as follows:

$$x_{D,h} = \frac{\varrho_h}{\alpha}, \quad (19)$$

where

$$\alpha = \dot{q}''_h - \sum_{k=1}^n B''_{h,k} \varrho_k - \left(\sum_{k=1}^n B''_{h,k} + B''_{h,h} \right) \varrho_h. \quad (20)$$

Using equation (19), one can estimate the equivalent internal reactance of a VPP. However, since (19) shows the same numerical issues as (5), we determine $x_{D,h}$ using the approach followed in (7) for the estimation of $M_{D,h}$. With this aim, we introduce the following differential equation:

$$T_x \dot{x}_{D,h} = \gamma(\alpha) (x_{D,h} \alpha - \varrho_h), \quad (21)$$

where $\gamma(\alpha)$ is defined by (8).

The rationale behind (21) is as follows. At the equilibrium point, $x_{D,h} \alpha - \varrho_h = 0$, whereas during a transient, $x_{D,h} \alpha - \varrho_h \neq 0$. Let us consider the case $x_{D,h} \alpha - \varrho_h > 0$. The sign of $\dot{x}_{D,h}$ is adjusted through the function $\gamma(\alpha)$ based on (8), in order to make $x_{D,h}$ converge to the actual reactance of the device. The sign of γ depends on the sign of α . If $\alpha > 0$, $x_{D,h}$ has to decrease, to also decrease $x_{D,h} \alpha - \varrho_h$ and converge to the equilibrium. In this case, $\dot{x}_{D,h} < 0$ and thus $\gamma(\alpha) = -1$. Otherwise, if $\alpha < 0$, $x_{D,h}$ has to increase to decrease $x_{D,h} \alpha - \varrho_h$ and thus $\gamma(\alpha) = 1$. Note also that the time constant of the differential equation T_x should be small enough to accurately track the time-varying reactance. A very small T_x , however, might generate numerical oscillations. Hence, T_x should be chosen in the time scale of the inertial response, i.e. $[10^{-2}, 10^{-1}]$ s.

The inertia of a VPP can finally be estimated using the set of equations (6)-(8), (20), (21). Thus, the proposed set of

equations to estimate the equivalent reactance and inertia, $x_{D,h}$ and $M_{D,h}$, of the VPP, can be summarized as follows:

$$\begin{aligned} \alpha &= \dot{q}_h'' - \sum_{k=1}^n B_{h,k}'' \varrho_k - \left(\sum_{k=1}^n B_{h,k}'' + B_{h,h}'' \right) \varrho_h, \\ T_x \dot{x}_{D,h} &= \gamma(\alpha) (x_{D,h} \alpha - \varrho_h), \\ \omega_{D,h} &= \Delta\omega_h - x_{D,h} \dot{p}_h', \\ T_M \dot{M}_{D,h} &= \gamma(\ddot{\omega}_{D,h}) (M_{D,h} \ddot{\omega}_{D,h} + \dot{p}_h'). \end{aligned} \quad (22)$$

It is relevant to note that the proposed estimator is able to capture the equivalent inertia provided by the VPP, regardless of the control design of its individual components.

To reduce the reactive power fluctuations and noise, filters are utilized for both q_h'' and ϱ_h . The real-time loop for the proposed inertia estimator based on (22) is shown in Fig. 2.

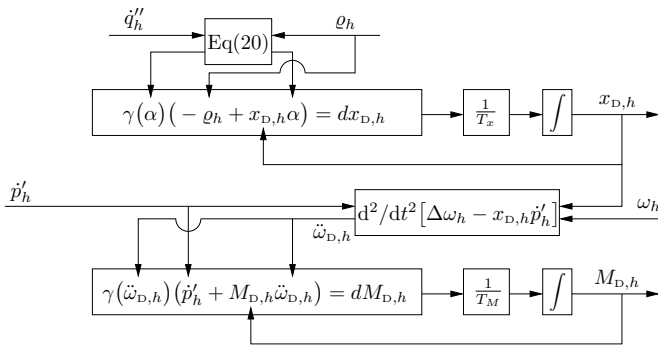


Fig. 2: Real-time loop for the proposed inertia estimator.

IV. CASE STUDY

This section investigates the performance and accuracy of the proposed on-line inertia estimation technique. The estimator is first evaluated for SMs based on simulations conducted using the well-known WSCC 9-bus system [15]. Then the applicability of the estimator for VPPs is assessed based on simulations conducted on a modified version of the same system. All simulation results are obtained using the power system analysis software tool Dome [16].

The single-line diagram of the test system is shown in Fig. 3. For all scenarios, SMs are represented by 4-th order (two-axis) models and are equipped with TGs and automatic voltage

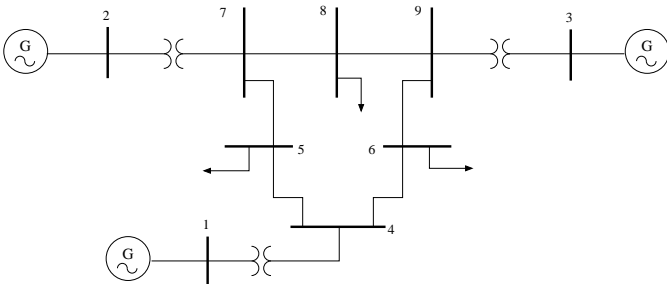


Fig. 3: WSCC 9-bus system.

regulators. We also assume that a Static Var Compensator (SVC) is installed at bus 8 of the network. Loads are modeled using the ZIP model, where the active and reactive power consumption, say $p_{L,h}$, $q_{L,h}$, are quadratic expressions of the bus voltage, as follows [17]:

$$\begin{aligned} p_{L,h} &= p_{zo} \left(\frac{v_h}{v_o} \right)^2 + p_{io} \frac{v_h}{v_o} + p_{po}, \\ q_{L,h} &= q_{zo} \left(\frac{v_h}{v_o} \right)^2 + q_{io} \frac{v_h}{v_o} + q_{qo}, \end{aligned} \quad (23)$$

where v_o , v_h are the nominal and measured voltage at the load bus, respectively; p_{zo}/q_{zo} , p_{io}/q_{io} , p_{po}/q_{qo} are the corresponding quota of constant impedance, constant current and constant power consumption, respectively. ZIP loads in this case study consist of 20% constant power, 10% constant current, and 70% constant impedance consumption [18].

Bus frequency estimations in this study are obtained using a Phase-Locked Loop (PLL). In particular, we employ the Synchronous Reference Frame PLL (SRF-PLL), which is one of the simplest and most commonly utilized schemes [19]. The fundamental-frequency model of an SRF-PLL is depicted in Fig. 4. It consists of a Phase Detector (PD) that is modeled as a pure delay; a Loop Filter (LF) that is a Proportional-Integral (PI) controller; and a Voltage-Controlled Oscillator (VOC) that is implemented as an integrator. In this scheme, θ_h is the phase angle of the voltage phasor at the measured bus.

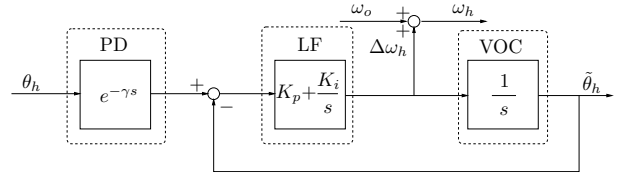


Fig. 4: Block diagram of the SRF-PLL.

The parameters of the SRF-PLL and of the inertia estimator are listed in Table I.

TABLE I: PLL and estimator parameters.

Device	Parameters
SRF-PLL	$K_p = 0.2$, $K_i = 0.01$
Estimator	$T_q = 0.05$ s, $T_\varrho = 0.001$ s, $T_x = 0.01$ s, $T_M = 0.004$ s

A. Single Synchronous Machine

This subsection provides a validation of the accuracy of the proposed method in estimating the inertia of a single SM, in particular of the machine connected to bus 2 of the WSCC 9-bus system (denoted as G2). The actual mechanical starting time of G2 is $M_{G2} = 12.8$ s.

We carry out a time domain simulation of the system twice, considering a 20% variation of the load connected to bus 6 at $t = 1$ s. In the first simulation the load is decreased and

in the second increased. Figure 5a shows how the estimated inertia compares to the actual mechanical starting time of G2. The proposed estimator can accurately capture the inertia of the SM. Note that the inertia estimator is initialized to zero, and thus the first second following the disturbance basically represents the training period of the estimator. Moreover, the estimated equivalent reactance x_{G2} of G2 obtained with the proposed method is shown in Fig. 5b, which indicates that the variation of the load has an impact on the estimation of x_{G2} . This in turn, slightly impacts on the final estimation of M_{G2} .

For completeness, we mention that for a single SM, the estimator in [12] is slightly more accurate than the one proposed in this paper. This result is to be expected as proposed method involves the estimation of two quantities, x_{G2} and M_{G2} , where the estimation of M_{G2} depends on that of x_{G2} . In [12], instead, the value of x_{G2} is assigned and assumed to be known accurately. On the other hand, if the value of x_{G2} is not correct, the method presented in [12] returns estimations with a systematic bias. The method proposed in this work is free from this potential bias as illustrated in Section IV-A.

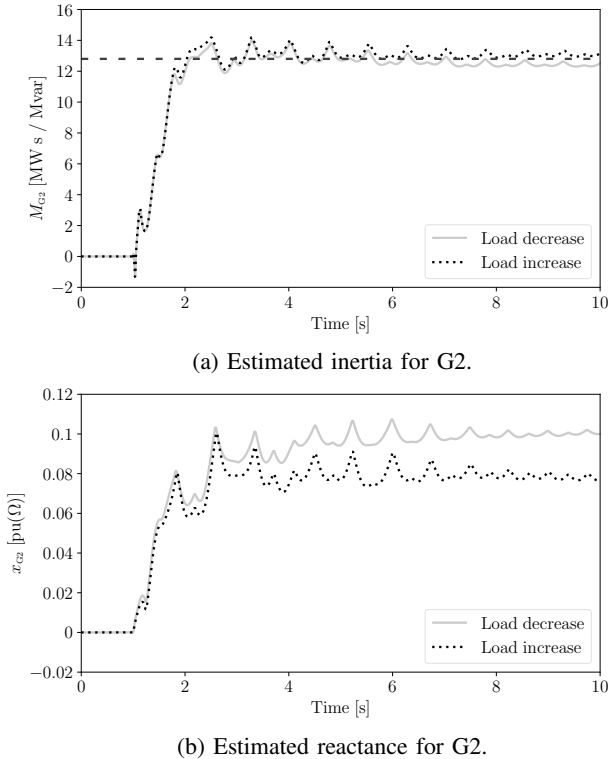


Fig. 5: 20% variation of load connected to bus 6.

Next, we study the impact of load models and TGs on the accuracy of the proposed estimator. In particular, the estimation using the ZIP load model is compared to the estimation when loads are represented using constant power (denoted as Constant PQ) and constant impedance (denoted as Constant Z) models. For each of these scenarios, we assume two cases: (i) all machines are equipped with TGs; and (ii) no machine is equipped with a TGs. The latter case is not realistic but it is considered for illustration purposes.

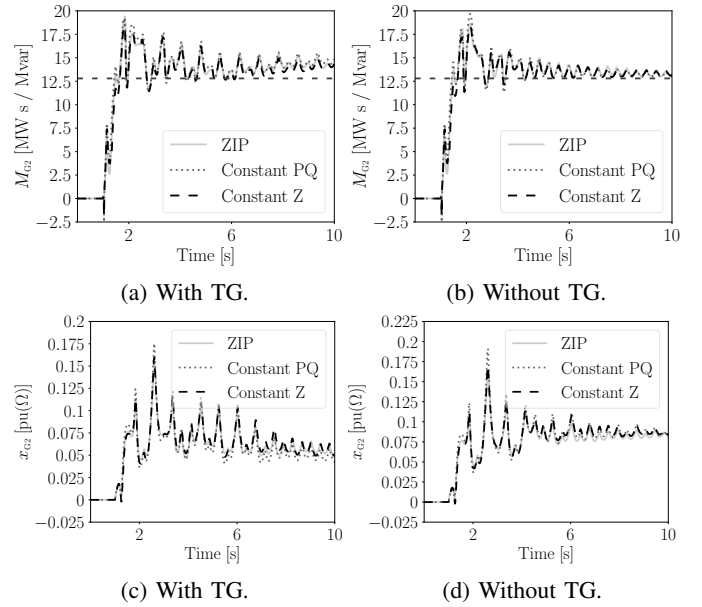


Fig. 6: 50% increase of load connected to bus 6. Impact of load model and TGs.

The disturbance consists in a 50% increase of the load connected to bus 6, occurring at $t = 1$ s. Simulation results are shown in Fig. 6. This figure shows that the inclusion of the PFC leads to a small increase of the deviation from the exact value of the inertia. This effect is stronger the larger is the power imbalance in the system, which is to be expected, due to the overlap in the time scales of the inertial response and the PFC. Regarding the effect on the estimation of load models, we see that is in general negligible, with constant power loads having the largest impact among the examined models.

B. Subnetwork with Multiple Machines

This subsection evaluates the proposed inertia estimation for multiple SMs. The original SM connected to bus 2 in Fig. 3 is substituted by a subnetwork with the same power injection. The subnetwork consists of two SMs in parallel with total starting time of 18.82 s, and one ZIP load with $p_{L,2,o} = 0.3$ pu, $q_{L,2,o} = 0.1$ pu. The examined contingency is the increase by 20% of the load connected to bus 8 at $t = 1$ s. The accuracy of the proposed inertia estimation method is compared to the method proposed in [12] and results are presented in Fig. 7. Figure 7a indicates that the proposed estimator can accurately track the inertia of the SMs in the subnetwork.

The method in [12] requires, for the estimation of the inertia, to assign a value to the equivalent internal reactance of the subnetwork. Apparently, for the simple topology examined in this example, i.e. two SMs in parallel, a proper selection of $x_{D,2}$ is simply the parallel of the transient reactances of the two machines, which yields $x_{D,2} = 0.07$ pu. However, for more complex topologies, comprising several nodes and devices of varying complexity, the selection is not straightforward. In Fig. 7 we show the effect on the estimator in [12] of choosing

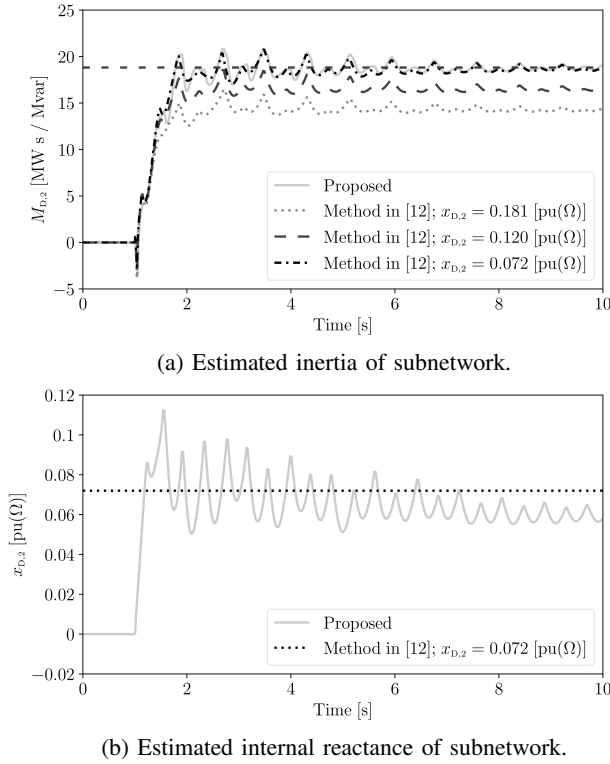


Fig. 7: 20% increase of load connected to bus 8.

different values for the equivalent reactance. In particular, apart from $x_{D,2} = 0.07$ pu, we also assume two more values, i.e. the internal reactance is set equal to the transient reactance of each of the SMs in the subnetwork, which gives $x_{D,2} = 0.12$ pu and $x_{D,2} = 0.18$ pu. Results indicate that an improper selection of $x_{D,2}$ has a significant impact on the accuracy of the inertia estimation. The estimation of the equivalent reactance provided by the proposed method is shown in Fig. 7b.

C. Virtual Power Plant

In this subsection, we apply the proposed method for the estimation of the equivalent inertia provided by a VPP. To this aim, the load at bus 6 is replaced by a VPP. The VPP consists of 8 buses at 38 kV and is connected to the transmission grid through an under-load tap changer type step down transformer. The VPP includes an ESS, as well as photovoltaic and wind generation. Stochastic fluctuations of wind speed in this study are modeled as an Ornstein-Uhlenbeck's process with Gaussian distribution [20]. The modified test system is depicted in Fig. 8. The parameters of the VPP are detailed in [21], [22].

The contingency in this subsection consists in the tripping of 20% of load connecting to bus 5, occurring at $t = 1$ s. The frequency, the estimated inertia and equivalent reactance of the VPP following the contingency are presented in Fig. 9, where we have considered various scenarios on the control strategies within the VPP, as follows: (i) with the ESS connected and with the VPP resources providing frequency control (denoted as FC_{VPP}), (ii) with the ESS but without FC_{VPP} , (iii) without the ESS but with FC_{VPP} , (iv) without ESS and FC_{VPP} .

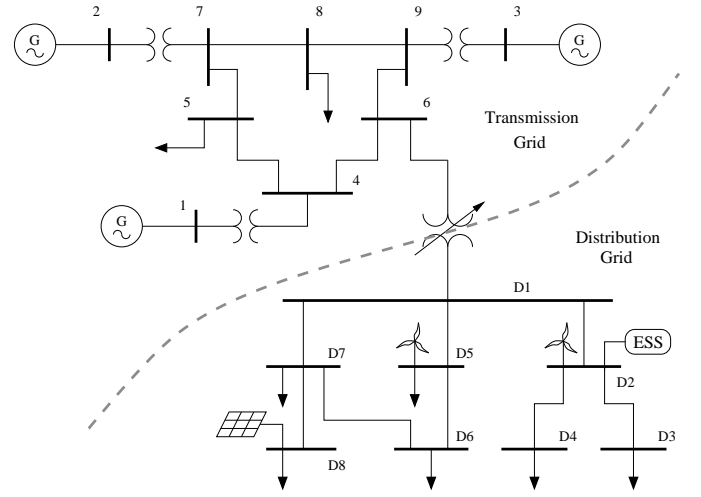


Fig. 8: WSCC 9-bus system modified to include the VPP.

Fig. 9b indicates that the VPP provides a time-varying inertia to the system, while the estimated equivalent reactance is also time-varying and might even take negative values (see Fig. 9c). As expected, the VPP without ESS nor frequency control practically does not provide any inertia support to the system. Moreover, the ESS and FC_{VPP} provide fast frequency regulation thus enhancing the inertial response of the VPP during the first instants after the contingency (see 9a).

We finally study the impact of stochastic fluctuations on the proposed inertia estimator. With this aim, we assume that the ESS is connected and the FC_{VPP} in operation, and a Monte Carlo analysis is carried out based on 500 simulations. Figure 10 shows the trajectories of $M_{D,6}$ obtained with all 500 tests, where μ and σ denote the mean value and the standard deviation. The stochastic fluctuation leads to some uncertainty on $M_{D,6}$. However, the deviation of the estimation from the mean value lies within an acceptable range.

V. CONCLUSIONS

This paper proposes an on-line inertia estimation method for VPPs. First, the paper provides a technique to estimate the internal equivalent reactance of any device connected to the grid, based on measurements of the reactive power and by using the concept of the complex frequency formula developed in [13]. Then, the estimated reactance is utilised for the estimation formula of the equivalent inertia of VPPs comprising a subnetwork and several distributed energy resources and loads. Simulations results indicates that the proposed method works well for synchronous machines. This builds up the trust on the results obtained with a VPP in various scenarios and considering different control strategies.

We will dedicate future work to further evaluate the proposed method under different disturbance scenarios and topologies, as well as to improve its accuracy, e.g. against the potential adverse effects due to the PFC provided by resources outside the VPP. Another relevant extension of this work is to explore relevant applications, including the deployment of the

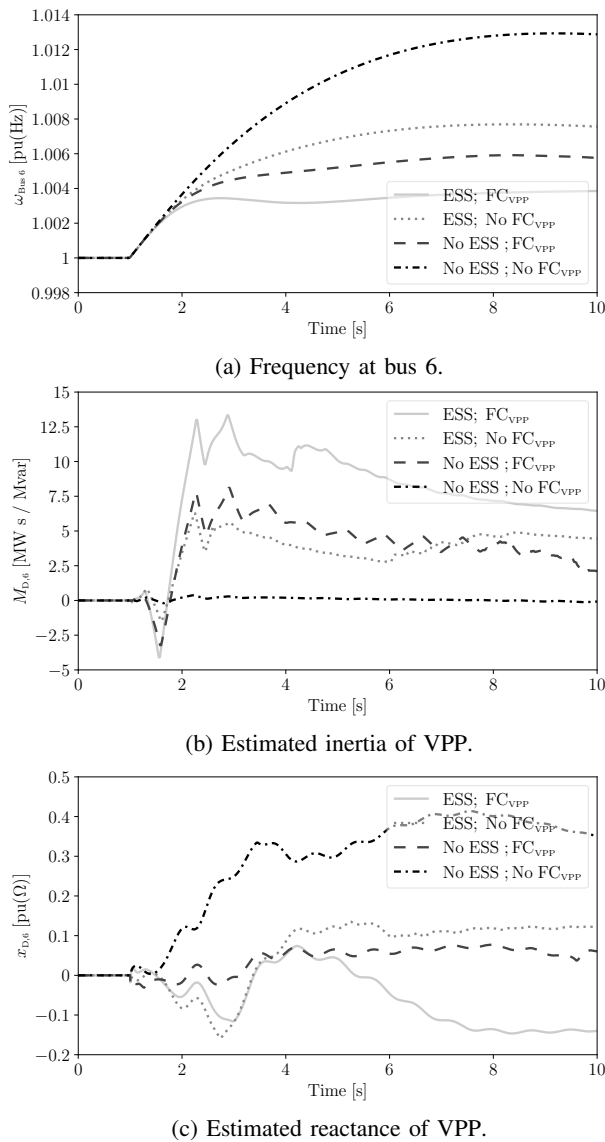


Fig. 9: 20% decrease of load connected to bus 5.

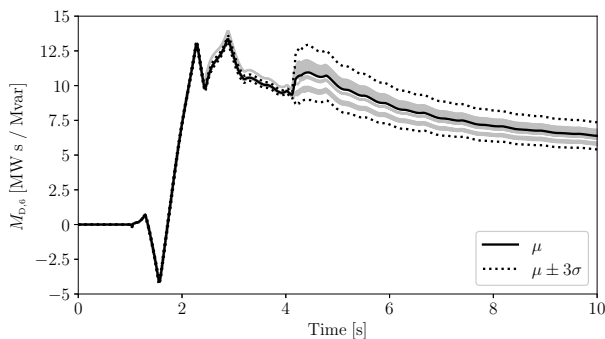


Fig. 10: Estimated inertia of VPP with ESS and FC_{VPP} ; Monte Carlo analysis.

equivalent estimated inertia to further improve the dynamic response of the power grid.

REFERENCES

- [1] E. Mashhour and S. M. Moghaddas-Tafreshi, "Bidding strategy of virtual power plant for participating in energy and spinning reserve markets – Part I: Problem formulation," *IEEE Transactions on Power Systems*, vol. 26, no. 2, pp. 949–956, 2010.
- [2] F. Milano, F. Dörfler, G. Hug, D. J. Hill, and G. Verbič, "Foundations and challenges of low-inertia systems," in *Power Systems Computation Conference (PSCC)*. Dublin, Ireland, 2018, pp. 1–25.
- [3] W. Zhong, J. Chen, M. Liu, M. A. A. Murad, and F. Milano, "Coordinated control of virtual power plants to improve power system short-term dynamics," *Energies*, vol. 14, no. 4, p. 1182, 2021.
- [4] T. Inoue, H. Taniguchi, Y. Ikeguchi, and K. Yoshida, "Estimation of power system inertia constant and capacity of spinning-reserve support generators using measured frequency transients," *IEEE Transactions on Power Systems*, vol. 12, no. 1, pp. 136–143, 1997.
- [5] P. M. Ashton, C. S. Saunders, G. A. Taylor, A. M. Carter, and M. E. Bradley, "Inertia estimation of the GB power system using synchrophasor measurements," *IEEE Transactions on Power Systems*, vol. 30, no. 2, pp. 701–709, 2014.
- [6] P. Wall, F. Gonzalez-Longatt, and V. Terzija, "Estimation of generator inertia available during a disturbance," in *2012 IEEE Power and Energy Society General Meeting*. IEEE, 2012, pp. 1–8.
- [7] P. Wall and V. Terzija, "Simultaneous estimation of the time of disturbance and inertia in power systems," *IEEE Transactions on Power Delivery*, vol. 29, no. 4, pp. 2018–2031, 2014.
- [8] J. Zhang and H. Xu, "Online identification of power system equivalent inertia constant," *IEEE Transactions on Industrial Electronics*, vol. 64, no. 10, pp. 8098–8107, 2017.
- [9] U. Tamrakar, D. Shrestha, M. Maharjan, B. P. Bhattarai, T. M. Hansen, and R. Tonkoski, "Virtual inertia: Current trends and future directions," *Applied Sciences*, vol. 7, no. 7, p. 654, 2017.
- [10] D. Chen, Y. Xu, and A. Q. Huang, "Integration of dc microgrids as virtual synchronous machines into the ac grid," *IEEE Transactions on Industrial Electronics*, vol. 64, no. 9, pp. 7455–7466, 2017.
- [11] F. Milano and Á. Ortega, "A method for evaluating frequency regulation in an electrical grid – Part I: Theory," *IEEE Transactions on Power Systems*, vol. 36, no. 1, pp. 183–193, 2020.
- [12] M. Liu, J. Chen, and F. Milano, "On-line inertia estimation for synchronous and non-synchronous devices," *IEEE Transactions on Power Systems*, vol. 36, no. 3, pp. 2693–2701, 2021.
- [13] F. Milano, "Complex frequency," *IEEE Transactions on Power Systems*, pp. 1–1, 2021.
- [14] P. Kundur, *Power System Stability and Control*. New York: McGraw-Hill, 1994.
- [15] P. W. Sauer and M. A. Pai, *Power System Dynamics and Stability*. Prentice hall Upper Saddle River, NJ, 1998, vol. 101.
- [16] F. Milano, "A Python-based software tool for power system analysis," in *Proceedings of the IEEE PES General Meeting*, Jul. 2013, pp. 1–5.
- [17] —, *Power System Modelling and Scripting*. London: Springer, 2010.
- [18] J. V. Milanović, K. Yamashita, S. M. Villanueva, S. Ž. Djokic, and L. M. Korunović, "International industry practice on power system load modeling," *IEEE Transactions on Power Systems*, vol. 28, no. 3, pp. 3038–3046, 2012.
- [19] G.-C. Hsieh and J. C. Hung, "Phase-locked loop techniques. A survey," *IEEE Transactions on industrial electronics*, vol. 43, no. 6, pp. 609–615, 1996.
- [20] F. Milano and R. Zárate-Miñano, "A systematic method to model power systems as stochastic differential algebraic equations," *IEEE Transactions on Power Systems*, vol. 28, no. 4, pp. 4537–4544, 2013.
- [21] W. Zhong, M. A. A. Murad, M. Liu, and F. Milano, "Impact of virtual power plants on power system short-term transient response," *Electric Power Systems Research*, vol. 189, p. 106609, 2020.
- [22] W. Zhong, T. Kërçi, and F. Milano, "On the impact of topology on the primary frequency control of virtual power plants," in *2021 IEEE Madrid PowerTech*. IEEE, 2021, pp. 1–6.